TRANSPORT PROPERTIES OF VISCOUS VORTEX RINGS

F. Kaplanski* and Ü. Rudi
Estonian Energy Research Institute, Paldiski mnt. 1, EE-0001 Tallinn, Estonia

*Conference Lecturer

ABSTRACT

This study involves the transport or stirring properties of viscous vortex rings. In order to take into account the Reynolds - number dependence, the method of entrainment diagrams is applied [1]. The system for pathlines of fluid particles is developed with the help of obtained analytical solution for a vortex ring. The idea of such approach is based on the property of this dynamical system to include complicated Reynolds - number dependence despite the fact that the linear solution of Navier-Stokes equations is used. Unsteady particle trajectories are examined as a bifurcation of an autonomous system with the initial Reynolds number as a parameter. It is shown that for small ratio of external and internal radiuses of the ring three regimes of particle motion exist and the pattern bifurcates at a two Reynolds numbers of 140 and 640.

I. INTRODUCTION

There are several problems in which stirring processes in a vortex ring are of direct relevance, and many others for which they provide a simple canonical representation of potentially more complicated processes. Examples range from the stirring processes in a rising atmospheric thermal and their implications for cloud formation, to the processes occurring during the interaction of a vortex ring with a premixed flame[2]. The interest in the processes of fluid stirring drives us to the Lagrangian approach based on the study of motion of an individual fluid particle **x** in a known Eulerian velocity field (**x**,**t**). As is shown in [1] such approach can be especially successful if description of the flow can be reduced to a self -similar form. In this case, the particle - path equations transform into an autonomous system in similarity coordinates. The aim of this paper is to use this approach for the viscous vortex ring.

II. MODEL OF A VISCOUS VORTEX RING

The flow is assumed to be axisymmetric and incompressible with constant density ρ and viscosity ν.

Figure 1 depicts schematic representation of a vortex ring in the cylindrical coordinates x,r.

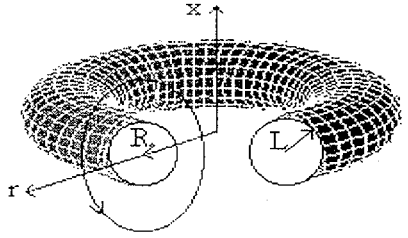

Fig.1

A solution for the limit $\mathrm{Re}\to 0$ is given by the expression for the vorticity [3]

$$\omega = \exp\left(-\frac{1}{2}\left(\sigma^2+\eta^2+\tau^2\right)\right) I_1(\sigma\tau), \qquad (1)$$

where the dimensionless variables are

$$\sigma=\frac{r}{L},\ \eta=\frac{x-x_0(t)}{L},\ \tau=\frac{R_0}{L},\ \omega=\frac{\varsigma}{\varsigma_0};\ L=(2M)^{1/2},\ \mathrm{Re}=\frac{\varsigma_0 L^2}{\nu} \qquad (2)$$

and I_1 denotes the first-order modified Bessel function of the first kind. The parameter $x_0(t)$ is the distance, which the vortex ring passes from the initial moment t_0, and R_0 determines the ring radius at t_0. The flow invariant is the impulse of vorticity

$$I = \pi\rho\int_0^{\infty}\int_{-\infty}^{\infty} r^2\varsigma\,dx\,dr \qquad (3)$$

with the help of which we can obtain

$$\varsigma_0 = \frac{2M}{(4\pi\nu t)^{3/2}R_0},\quad M=\frac{I}{\rho}, \qquad (4)$$

$$\mathrm{Re}=\frac{M}{2(\pi\nu)^{3/2}(t)^{1/2}R_0}=\frac{M\tau}{2^{1/2}(\pi)^{3/2}\nu R_0^2}=\frac{\mathrm{Re}_0\,\tau}{\sqrt{2\pi}}, \qquad (5)$$

where $\mathrm{Re}_0=\frac{\Gamma_0}{\nu}$ is the initial Reynolds number and $\Gamma_0=\frac{M}{\pi R_0^2}$ the initial circulation.

The mixing processes of ring are determined by interaction of strain and diffusion and are described by the advection-diffusion equation. A linear solution of this equation for the limit $\mathrm{Re}\to 0$ and for the Schmidt number $\mathrm{Sc}=\frac{\nu}{D}=1$ is given by the expression for a passive scalar

$$C_1 = \exp\left(-\frac{1}{2}\left(\sigma^2+\eta^2+\tau^2\right)\right) I_0(\sigma\tau), \qquad (6)$$

where $C_1=\frac{C}{C_0}$, D denotes the coefficient of diffusion and C_0 is determined by condition of the conservation of C. The contour lines of C_1 for this case represent shapes which are symmetrical about the η-axes. In accordance with results of the numerical calculations the contour lines of C_1 lose this symmetry with the increase of Re due to nonlinearity. The applied approach allows us to determine the range of Re, at which the contribution of the nonlinearity is significant, and to obtain particle trajectories for this interval.

III. FIELD OF THE STREAMFUNCTION

The vorticity is related to the streamfunction Ψ by the equation

$$\frac{\partial^2\Psi}{\partial r^2}+\frac{\partial^2\Psi}{\partial x^2}-\frac{1}{r}\frac{\partial\Psi}{\partial r}=-r\,\varsigma. \qquad (7)$$

Boundary conditions follow from the symmetry about the x axis and the decay of Ψ at the infinity

$$\Psi(0,x)=0,\ (r=0),\ \Psi\to 0,\ \left(x^2+r^2\right)^{1/2}\to\infty. \qquad (8)$$

The dimensionless streamfunction is $\Phi=\dfrac{\Psi}{\varsigma_0 L^3}$.

The Fourier - Hankel integral transforms of the vorticity ω and of the function $f=\dfrac{\Phi}{\sigma}$ from the equation (7) are:

$$\bar{\omega}=\exp\left(-\frac{\mu^2+\alpha^2}{2}\right)J_1(\tau\mu),\ \bar{f}=\frac{\exp\left(-\frac{\mu^2+\alpha^2}{2}\right)}{\mu^2+\alpha^2}J_1(\tau\mu), \qquad (9)$$

where J_1 denotes the first-order Bessel function. Using the inverse Fourier- Hankel integral transform for $\bar{f}$, we obtain Ψ as follows

$$\Psi=\frac{2\varsigma_0 L^3\sigma}{(2\pi)^{1/2}}\int_0^\infty\int_0^\infty\frac{\mu\exp\left(\frac{-\mu^2-\alpha^2}{2}\right)}{\mu^2+\alpha^2}J_1(\tau\mu)J_1(\sigma\mu)\cos(\alpha\eta)\,d\mu\,d\alpha.$$

The integration with respect to α presented in [4] gives

$$\int_0^\infty\frac{\exp\left(\frac{-\alpha^2}{2}\right)}{\mu^2+\alpha^2}\cos(\alpha\eta)\,d\alpha=\left(\frac{\pi\exp(\frac{\mu^2}{2})}{4\mu}\right)F(\mu,\eta), \qquad (10)$$

where $F(\mu,\eta)=G(\mu,\eta)+G(\mu,-\eta), G(\mu,\eta)=\exp(\eta\mu)\left(1-\mathrm{erf}\left(\frac{\mu+\eta}{\sqrt{2}}\right)\right)$

and erf(z) is the error function. Thus, we have the expression for Ψ in the form of a single integral

$$\Psi=\frac{M\sigma}{4\pi R_0}\int_0^\infty F(\mu,\eta)\,J_1(\tau\mu)J_1(\sigma\mu)\,d\mu \qquad (11)$$

and the two velocity components in dimensionless form inside the moving vortex ring become

$$v_t=-\frac{1}{\sigma}\frac{\partial\Phi}{\partial\eta}=-\frac{\sqrt{\pi}}{2\sqrt{2}}\int_0^\infty\mu\{-G(\mu,-\eta)+G(\mu,\eta)\}J_1(\tau\mu)J_1(\sigma\mu)d\mu,$$

$$u_t=\frac{1}{\sigma}\frac{\partial\Phi}{\partial\sigma}=\frac{\sqrt{\pi}}{2\sqrt{2}}\int_0^\infty\mu^2F(\mu,\eta)\,J_1(\tau\mu)J_0(\sigma\mu)d\mu. \qquad (12)$$

The obtained vorticity distribution (1) transforms into Phillips' result [5] in long time limit and at $t\to 0$ it tends to delta-function. The behavior of the evaluated streamfunction (11) for early times and in long time is consistent with this statement and at $t\to 0$ it tends to circular vortex line. The expression for a circular line vortex in our designations is written as

$$\Psi_*=\frac{M\sqrt{\sigma}}{\left(2\pi^2\sqrt{\tau}\right)R_0^2}\left\{\left(\frac{2}{k}-k\right)K(k)-\frac{2}{k}E(k)\right\},k^2=\frac{4\tau\sigma}{\eta^2+(\tau+\sigma)^2}, \qquad (13)$$

where K and E are elliptical integrals of the first and second kind, respectively.

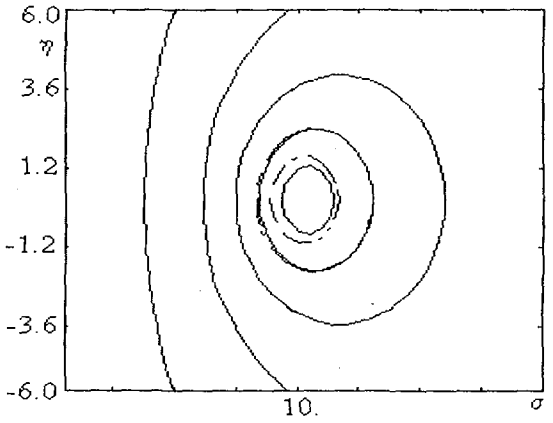

Fig.2 Comparison of Ψ with Ψ_*. Solid lines represent the contour plots of 90, 70, 50, 30 and 10% of Ψ_{max} -Eq.(11) and broken lines the same values of circular line vortex - Eq.(13) for $\tau=10$.

Formally we can describe the starting ring's motion for $t\to 0$ using the obtained solution when the initial Reynolds number Re_0 is very small. But a circular line vortex is a limiting solution of the full Navier-Stokes equations and usually used for the description of a starting ring for any Reynolds numbers. The variable τ is the ratio of external and internal radiuses for the initial stage of a vortex ring development. These properties permit to consider expressions (12) as approximations for early times of ring's evolution for fixed τ.

IV. ENTRAINMENT DIAGRAMS

The equations for particle paths are

$$\dot{x}=\frac{1}{r^k}\frac{\partial\Psi}{\partial r}+U(t),\ \dot{r}=-\frac{1}{r^k}\frac{\partial\Psi}{\partial x}, \qquad (14)$$

where the dot denotes the time derivative and $U(t)=\dfrac{dx_0(t)}{dt}$ is the velocity of the frame moving with the vortex ring. The corresponding system in dimensionless variables σ, η is

$$\frac{d\sigma}{ds}=-\frac{\sigma}{2}+\frac{2\sqrt{2}}{\sqrt{\pi}}\frac{Re_0\,\tau}{8}v_t,\ \frac{d\eta}{ds}=-\frac{\eta}{2}+\frac{2\sqrt{2}}{\sqrt{\pi}}\frac{Re_0\,\tau}{8}u_t, \qquad (15)$$

where s= ln t. The system (15) is considered as an autonomous system with the Reynolds number Re_0 as a parameter for fixed values of τ. The pattern of particle displacements in coordinates σ,η is independent of velocity for a moving observer [1]. The structure of the flow is examined by finding and classifying critical points of (15); points (σ_c, η_c) at which both right-hand sides of (15) are equal to zero. In spite of the trivial Reynolds - number dependence of the solution (1,11), which is valid

for $Re \to 0$, the system (15) exhibits a Reynolds - number dependence that is quite complex. We expect that the linear solution in system (15) behaves similarly to the nonlinear solution. In [6] this approach was applied to the problem of an impulsively started, axisymmetric, laminar jet. Figure 3 (a, b) shows particles trajectories (15) for two values of the Reynolds number and for $\tau=10$. For small Reynolds number, pathlines converge to a single node, which lies on the axis η. All trajectories for this regime are similar: the particles are involved due to diffusion. At a Reynolds number of $Re_0=140$ new critical points occur - a two saddles and two foci lying symmetrically to either side of axis η. Particles trajectories are divided into two parts: some of them as well as earlier are involved due to diffusion when other part begins to be involved in the core of ring due to growth of concentration of vorticity. At a Reynolds number of $Re_0=640$ saddles disappear and all the trajectories begin to be directed towards the centre of vortex ring.

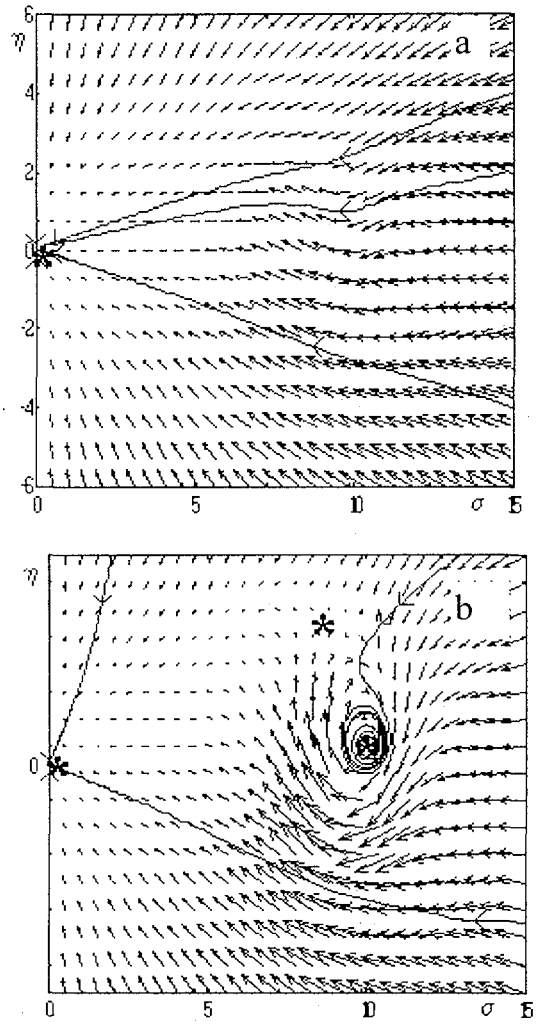

Fig.3 Particle trajectories for $Re_0=40$ (a) and 200(b) presented by (15) for $\tau=10$, critical points are marked by *.

Using the Hankel's integral transforms (9) and Parseval's theorem we can calculate the translation velocity of the ring U(t) [7] and particles trajectories in a system in which there is a relative wind, -U

$$\frac{d\sigma}{ds} = -\frac{\sigma}{2} + \frac{2\sqrt{2}}{\sqrt{\pi}} \frac{Re_0 \tau}{8} v_t,$$

$$\frac{d\eta}{ds} = -\frac{\eta}{2} + \frac{2\sqrt{2}}{\sqrt{\pi}} \frac{Re_0 \tau}{8} u_t - \frac{Re_0}{8\pi} U_*, \qquad (16)$$

$$U_* = \int_0^\infty \left\{ \pi(1-erf(\mu))(1-6\mu^2) + 6(\pi)^{1/2} \mu \exp(-\mu^2) \right\} J_1^2(\tau\mu) d\mu \qquad (17)$$

Here as the translation velocity of a ring the speed of the three -dimensional vortex centroid is applied[8].

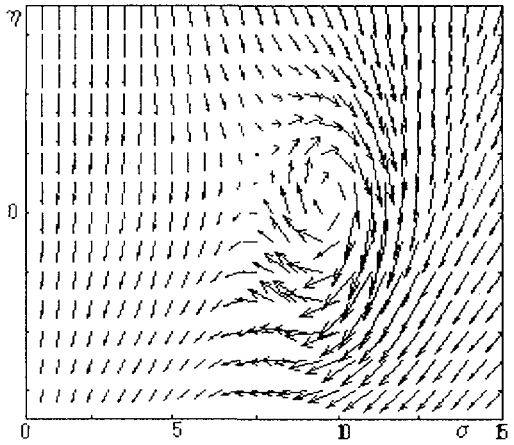

Fig.4. Velocity vectors for $Re_0=500$ presented by (16) for $\tau=10$.

Velocity vectors in this system give evident representation about particle motion (Fig.4) and are in good agreement with results of direct numerical simulation of a laminar vortex ring [9]. The carried out analysis shows that with the increase of Reynolds numbers the particle trajectories take the forms conducting to formation of a wake.

This work was supported by Estonian Scientific Foundation (Grant No.2213).

References

[1] B. J. Cantwell, Ann. Rev. Fluid Mech. **13**, 158 (1981).
[2] K. B. Southerland, J. R. Porter III, W. J. A. Dahm, and K. A. Buch, Phys. Fluids A **3**, (5),1385, (1991).
[3] A. A.Berezovski, and F. B.Kaplanski, Fluid Dynamics, **22**, 832, (1988).
[4] A. P Prudnikov, Yu. A. Brychkov, and O. I. Marichev, *Integrals and Series* (in Russian). - M., Nauka, (1983).
[5] O. M. Phillips, Proc. Cambridge Phil. Soc. **52**, 135 (1956).
[6] B. J. Cantwell, J. Fluid Mech. **104**, 369 (1981).
[7] F.B. Kaplanski, Proc. Estonian Acad. Sci. Engng., **3**, 171, (1997).
[8] P. G. Saffman, *Vortex Dynamics*,-Cambridge University Press, 371 (1992).
[9] S. James and C. K. Madnia, Phys. Fluids **8**, 9 (1996).